Review Article

Fedor Grigoriev*, Vladimir Sulimov and Alexander Tikhonravov

Simulation of the optical coating deposition

Abstract: A brief review of the mathematical methods of thin-film growth simulation and results of their applications is presented. Both full-atomistic and multi-scale approaches that were used in the studies of thin-film deposition are considered. The results of the structural parameter simulation including density profiles, roughness, porosity, point defect concentration, and others are discussed. The application of the quantum level methods to the simulation of the thin-film electronic and optical properties is considered. Special attention is paid to the simulation of the silicon dioxide thin films.

Keywords: deposition simulation; molecular dynamics; oxide films; thin-film deposition; thin-film properties.

1 Introduction

The first simulations of thin-film growth were performed more than 30 years ago [1, 2]. In these simulations, deposited atoms were considered as two-dimensional hard disks, and the substrate was represented as a strip consisting of the same disks as deposited ones. Despite its obvious simplicity, this model was able to qualitatively describe the structural properties of growing films, among them such important property as the columnar structure of thin film.

Because of the tremendous progress in high-performance computing, the simulation of thin-film growth gained a new interest in recent years. The atomistic simulation of optical layers having technologically sensible thicknesses of about a quarter of visible light wavelength is possible now using modern supercomputer facilities.

*Corresponding author: Fedor Grigoriev, Research Computing Center, Moscow State University, Leninskie Gory, 119992 Moscow, Russia, e-mail: fedor.grigoriev@gmail.com
Vladimir Sulimov and Alexander Tikhonravov: Research Computing Center, Moscow State University, Leninskie Gory, 119992 Moscow, Russia

The goal of this simulation is to provide insight onto dependencies of the film properties on deposition parameters such as deposited atom energy, substrate temperature, deposition rate, and angular distribution of the deposited atom flow.

In the simulation process, deposited films are represented by microscopic atomistic clusters. The numbers of atoms in these clusters and cluster dimensions are essentially dependent on the simulation approaches, which can be divided into quantum and classical ones. The most fundamental and time-consuming quantum chemistry (QC) simulation level is able to provide calculations of the optical and electronic properties of small clusters consisting of no more than several hundreds of atoms. Classical approaches provide calculation of structural and mechanical thin-film properties, but at the same time, they have a limited potential in optical property calculations because the light interaction with matter requires description at the quantum level.

The most essential features of the above-mentioned methods used for the simulation of thin-film growth and respective simulation software are considered in Sections 2 and 3, respectively. The applications of these methods, mainly classical molecular dynamics (MD), to the simulation of structural and mechanical thin-film properties are discussed in Sections 4 and 5. Simulations of optical and electronic thin-film properties are briefly considered in Sections 6. The final conclusions are given in Section 7.

2 Simulation methods

2.1 Input data for the simulation

In the classical simulation of the thin-film production, the following data are used as input data: parameters characterizing the beam of deposited particle parameters of the residual gas in a vacuum chamber, substrate temperature, etc. Unfortunately, such important input data as energy and velocity distributions of deposited particles and flux density are hardly available now for the most part of deposition processes.

There are two ways to handle this problem. The first one is based on the development of multi-scale models

[3] that are able to simulate interactions of ion beam with target and resulting energy and velocity distribution of atoms arriving at the substrate. The second way is the investigation of the dependence of the simulation results on various parameters of the deposition process. In this case, the characteristic values of the deposition parameters should be taken from the intervals that are typical for the simulated deposition techniques. For instance, for the low-energy deposition techniques like thermal evaporation, the characteristic values of deposited particle energy should be taken around 0.1 eV, while for the high-energy techniques like ion beam sputtering (IBS), the energy of the sputtered atoms may achieve several tens of eV.

2.2 Classical molecular dynamics and Monte-Carlo methods

In frame of the full-atomistic approaches every atom of the simulation cluster is considered as a force center interacting with other atoms in accordance with the chosen expressions for the potential energy of interatomic interaction. In the case of MD simulation processes atoms of the growing film move accordingly to the Newton's laws. In the case of Monte-Carlo (MC) method atoms move in agreement with the Metropolis scheme [4]. MD and MC algorithms are able to perform numerical experiments with millions of atoms and film thicknesses of more than hundred nanometers [5] at the modern high performance supercomputers. Time intervals of MD and MC modeling are limited by tens of nanoseconds and for this reason these modeling methods are not suitable for the simulation of such long-time processes as the surface diffusion. However, in the very recent years the combined MD and MC atomistic technique providing an essential acceleration of simulation was proposed [6]. In perspective this technique can be applied for optical coatings growth simulation.

Full-atomistic MD and MC approaches for deposition simulation are organized as a step-by-step procedure that, in general, consists of the following steps:

1. Substrate preparation. Both crystalline [7–9] and glassy or amorphous [10–16] structures are used as substrates. The annealing procedure can be used to prepare the glassy substrate from the crystalline structure [14].
2. Deposited atoms are injected into random positions above the substrate surface (Figure 1). Initial velocities are directed to the substrate according to the angular distribution of the deposited atom velocities.
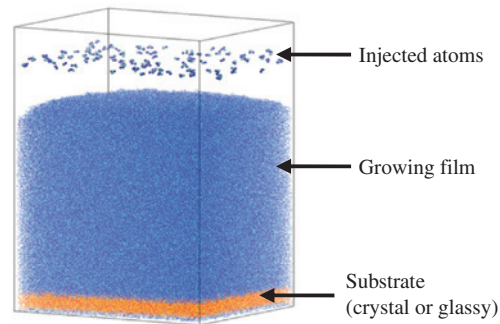

Figure 1: Simulation box structure.

Velocity values are specified accordingly to the energy distribution of the deposited particles, that is, either discrete [8, 10–15] or continuous [3].

3. MD (MC) simulation starts from the described configuration. As a rule, the NVT (constant number of particles, volume, and temperature) ensemble with the periodic boundary conditions is used at this simulation step. Also, the NVE (constant number of particles, volume, and energy) ensemble is used for thermal equilibration before NVT simulation [3, 8].
4. Steps 2 and 3 are repeated until the growing film thickness achieves a specified value.

This scheme was applied to the simulation of the silicon dioxide film deposition [7, 8, 10–14] as well as titanium dioxide [9], and other material [17] deposition.

The choice of the force field describing the interatomic interactions is one of the key issues in the classical atomistic simulation. Usually, the two-body interatomic potentials [18–22] are used for the thin-film growth simulation. In this case, the potential energy of the system is represented as the sum of terms depending on the distances between the pairs of interacting force centers. These terms are the electrostatic and the Van-der-Waals contributions. The first is the Coulomb interaction of point charges centered at the atoms. For the Van-der-Waals contribution, the Morse potential [23] was used for silica in Refs. [18, 19, 24, 25] and for TiO_2 [26]. The Lennard-Jones potential was applied for the silicon dioxide thin-film simulation [10–14] as well as for Si-(ZrCu) films [27]. In Ref. [17], the pairwise ionic potential was applied to the study of the Mg–Al–O thin-film deposition.

More sophisticated many-body potentials [28–31] were also used for the deposition process simulation [16]. The polarizable potentials were proposed to study the deposition of Ti_xO_y clusters with an impact energy of up to 40 eV onto a rutile substrate [32, 33].

The force field parameters are defined either from the quantum chemistry calculations [34–36] or from the fitting procedure comparing the calculated and experimental condense-phase properties. In Ref. [37], the *ab initio*-based force field was adapted for the condense-phase simulation and was applied for the simulation of the Ni film formation on the silicon dioxide substrate.

The universal ReaxFF force field based on the parameterization of the density functional theory (DFT) quantum chemistry calculations was developed in the recent year [38–40]. The ReaxFF has a functional form allowing one to describe the chemical bond formation and dissociation in terms of bond-order parameter depending on the interatomic distances. As the bond formation is an important component of the film growth process, the ReaxFF looks promising for the simulation of the deposition processes.

The following parameters are usually used in classical MD simulations of the silica deposition process [10–15]: the time step of the MD modeling is 0.5 fs, duration of one deposition cycle (step 3 in the algorithm described in this section) is 4–6 ps for NVT simulation. The duration of the NVE simulation is equal 1 ps [8]. The Berendsen thermostat [41] is used to keep the simulation box temperature constant. The electrostatic component of the interatomic energy is calculated using the particle mesh Ewald [42] method.

2.3 Kinetic Monte Carlo

In the above section, we joined discussions of the MD and MC methods because both methods have similar thermodynamic background and describe processes at the same level of sophistication. The kinetic Monte Carlo (kMC) stays separately and requires specifying the transition rates between the initial and possible final states of the system. These rates should be obtained from the results of the simulation using other methods such as MD and MC, mentioned in Section 2.2.

The kMC approach is specially oriented to the simulation of rare events. This approach is not accurate enough for the description of fast processes such as collisions of high-energy deposited atom with the substrate and the film, but it is suitable for the simulation of long-time processes like the diffusion of deposited atoms on the growing film surface. The kMC algorithms are able to simulate the processes having a duration of hundreds and thousands of seconds in the clusters consisting of millions of atoms [43, 44].

The kMC was applied for the simulation of Cu thin film growth [45, 46]. The diffusion of atoms on the growing surface was taken into account in the frame of the applied

model. The Morse potential was used for the calculation of interatomic potential energy with parameters that are defined in Refs. [24, 47]. The film density dependence on the substrate temperature was investigated in Ref. [45]. The multi-scale approach including the kMC simulation level was developed in Ref. [3] and was applied for the simulation of TiO_2 thin-film deposition. The density and roughness dependencies on the number of deposited atoms were investigated. In these simulation experiments, the maximum number of deposited atoms achieved two million.

2.4 Quantum methods

The QC approaches are used for the simulation of optical and electronic thin-film properties. As the QC modeling requires a lot of computational recourses, the simulation cluster dimensions are essentially smaller than those in the case of the MD simulations (Figure 2). The atomic positions in the QC cell should be optimized before the optical and electronic parameter calculations.

In Ref. [3], the quantum chemistry approach was applied for the optical property calculation of the resulting classical MD TIO_2 films. The stoichiometric TIO_2 supercell structure consisting of 96 atoms was prepared from the deposited film. All simulations were performed using the Vienna *ab initio* simulation package [48]. The electronic correlation and the exchange interaction were considered at the density functional theory level [49] in the frames of the PBE generalized gradient approximation [50] and the hybrid functional HSE06 [51].

The self-consistent charge density-functional-based tight-binding (DFTB) method was used in Ref. [52] for the simulation of the highest occupied molecular orbital–lowest unoccupied molecular orbital (HOMO–LUMO) gap and the electronic density of the states of the TIO_2 clusters.
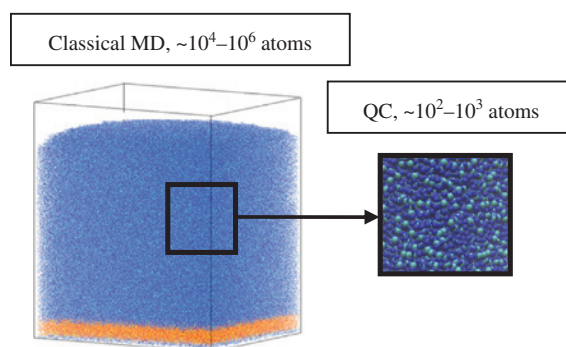

Figure 2: Comparison of the QC and classical MD simulation levels.

2.5 Other methods

In Ref. [53], the simplified approach referred to as the discrete approach was proposed. This approach describes the growing film as a set of sites that can be either empty or occupied by atoms [53]. The discrete approach is suitable for simulations of crystalline substrate and films. Several models of the deposition process – random, ballistic, and solid on solid – were considered [53]. In the frames of these models, every injected atom was deposited at a random position of a regular network representing the film surface. The models differ by equations describing the height dependence of a network site on the deposition time. In the simplest case of random deposition without diffusion, the model has an analytical solution predicting the unlimited surface roughness growth with the increase in the number of deposited atoms.

In Ref. [54], the simulation of the SiO_2 thin-film deposition was performed based on the assumption that silicon oxidation on the growing film surface can be described in terms of Brownian motion (three-dimensional random walk) of oxygen atoms. The probability of oxygen atoms moving from one local minimum to another was calculated as $\exp(-E/k_B T)$, where E is the activation energy. Moving was performed if the probability was greater than a random value in the interval [0; 1]. This scheme is close to the Metropolis algorithm that is widely used in MC simulations.

The dependence of the nanostructured TiO_2 film thickness on the deposition conditions was studied with the help of the artificial neural network (ANN) and regression method [26]. The ANN was used to determine the relationships between the deposition parameters and the deposited film properties. The author of Ref. [26] concluded that the application of the ANN in combination with MD simulations allows one to reduce the number of experiments.

2.6 Interface between different theory levels

One of the main tasks of the thin-film growth modeling is providing a proper interface between the different simulation levels. The problem is that the most accurate QC level providing the calculations of the key thin-film parameters (refractive index, electronic density gap, and so on) can be applied only to small clusters consisting of no more than several hundreds of atoms. The concept of the virtual coater [55] was proposed to solve the problem. The idea is to combine simulation techniques having different length scales to a multiple scale model. The corresponding approach is outlined in Ref. [55]. The vacuum chamber geometry, ion source, and target parameters were the

input data for the first simulation level. The output of this level (deposited atom energy and velocity distribution, density of their flow, charges of the deposited atoms, and so on) were then used as the input data for the classical simulation approaches: MD, MC, and kMC. The structural parameters (density, point defect concentration, porosity, and structural ring distribution) can be used to prepare the simulation cells for the QC level. The first results of the application of this scheme in studying titanium oxide films is presented in Ref. [3].

3 Software for the thin-film growth simulation

The software for the film growth simulation should be chosen taking into account its potential for reproducing the main features of a real deposition process: injections of deposited atoms, atomic collisions with a film and substrate-film interface, formation of transition layers between film and vacuum, and specific boundary conditions.

The quantum molecular dynamics simulations of the structural, electronic, and optical properties of deposited film can be performed using the Vienna Ab Initio Simulation Program (VASP) (University of Vienna, Faculty of Physics, Vienna, Austria) [48]. The many-body quantum problem can be considered in the VASP in the frame of the density function theory, Hartree-Fock approximation, and perturbation theory (second-order Møller-Plesset). At the same time, a direct simulation of the deposition process in the VASP requires an adequate description of the transition layer between condense matter and vacuum.

The large-scale atomic/molecular massively parallel simulator (LAMMPS) (Sandia National Laboratories, US Department of Energy laboratory, Livermore, CA, USA) (http://lammps.sandia.gov/) is suitable for the thin-film growth simulation using the classical MD approach. The LAMMPS provides step-by-step injections of the deposited atoms into the simulation area. Different pairwise and polarizable force fields are implemented in the LAMMPS.

Groningen machine for chemical simulations (GROMACS) (Department of Biophysical Chemistry, University of Groningen, Groningen, Netherlands) [56], Not another molecular dynamics program (NAMD) (Beckman Institute of the University of Illinois, Urbana-Champaign, CA, USA) (http://www.ks.uiuc.edu/), and DLPOLY (A general-purpose parallel molecular dynamics simulation package) [Science and Technology Facilities Council (STFC), Daresbury, UK] [57] software packages can be also used for the thin-film deposition simulation

on the classical atomistic level despite the fact that both programs were initially oriented to the organic molecule modeling. All mentioned programs are well paralleled and can be installed on the supercomputers.

Simulations at the kMC level can be performed using the three-dimensional kinetic Monte Carlo code nanoscale modeling (NASCAM) (University of Namur, Department of Physics, Namur, France) (http://www.unamur.be/sciences/physique/pmr/telechargement/logiciels/nascam). This code was specially developed for the simulation of deposition, diffusion, nucleation, and growth of films.

4 Structural properties

4.1 Density

The results of the silicon dioxide density calculations using the classical MD simulations with different force fields are summarized in Table 1.

It is seen from Table 1 that the most part of the applied force fields reproduce the experimental value of the silicon dioxide glassy density (this value is equal to 2.2 g/cm^3). It is likely that the high density value of 2.58 g/cm^3 reported in Ref. [58] for the Beest Kramer and van Santen (BKS) force field [21] is connected with the BKS fitting scheme that is oriented to the calculations of the crystalline cell parameters.

Simulations of the thin-film deposition processes in the frame of the deposited films of silica (DESIL) force field [10–14] show that the deposited film density is somewhat higher than the density of glassy silica. These simulations also show that the film density is higher when the energy of the deposited silicon atoms is higher.

Thermal annealing results in the essential reduction of the densities of the deposited SIO$_2$ films (see the bottom row of Table 1). This result is in a good agreement with the experimental data [60].

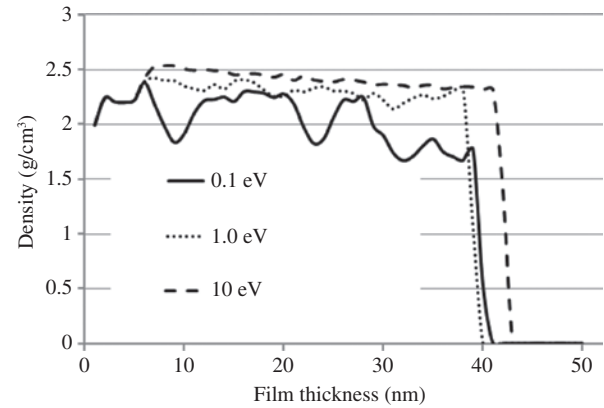**Figure 3:** Density profiles of the deposited SiO$_2$ films.

The density profiles of the deposited silicon dioxide films are shown in Figure 3. Simulations were performed in the frame of the DESIL force field for the three different values of silicon atom energy. Silica glass substrate was prepared from α-quartz by heating it from 300 K to the temperature above the quartz melting point followed by quenching in the MD simulation with GROMACS [56]. Every deposition cycle was simulated in the NVT (constant number of atoms, volume, and temperature) ensemble. The deposition temperature was equal to 300 K, and the initial velocities of the oxygen atoms corresponded to 0.1 eV. Essential fluctuations of the film density were observed in the case of low-Si atom energy. The increase in deposition energy results in a smoother density profile.

The density profiles of the silicon dioxide thin films for the temperature values in the interval from 3400 K to 5200 K are reported in Ref. [61]. The BKS force field [21] was used for the simulation. The maximum cluster size in Ref. [61] achieved 2.7 nm. The density fluctuations with amplitudes up to 0.2 g/cm^3 were observed. The thickness of the transition layer between the film and vacuum achieved 0.5–0.7 nm.

Table 1: Density ρ (g/cm^3) of silicon dioxide glassy and thin films.

Glassy								
ρ	2.18 [34]	2.21 [18]	2.58 [21]	2.3[a] [35]	2.2[a] [58]	3.0[a,b] [59]	2.42[a] [30]	2.14 [10]
Films								
E	0.1		1		5		10	
ρ	2.06		2.29, 1.95 [8]		1.98 [8]		2.41, 2.1 [8]	
ρ[c]	2.03		2.2				2.25	

E (eV), energy of deposited silicon atoms.
[a]Data from Ref. [58].
[b]Density of SIO$_2$ nanoparticles.
[c]Results for the annealed films. Annealing temperature and simulation duration were equal to 1300 K and 3 ns, respectively. The annealing simulation procedure is described in Ref. [14].

The dependence of the TIO_2 film density on the number of deposited atoms was investigated in Ref. [3] using the kMC approach. The MA pairwise potential [31], including the Coulomb and Buckingham terms, was used. It was found that the density reduces with the growth of the deposited atom number N (the N values of up to ~10^6 were considered). It was also found that the density reduces from 3.4 to 2.7 g/cm³ with the growth of incidence angle from 0° to 50° in the case of the TI atom energy of 0.1 eV. The density increased approximately for 0.6 g/cm³ when the TI atom energy was increased from 0.1 eV to 10 eV [3].
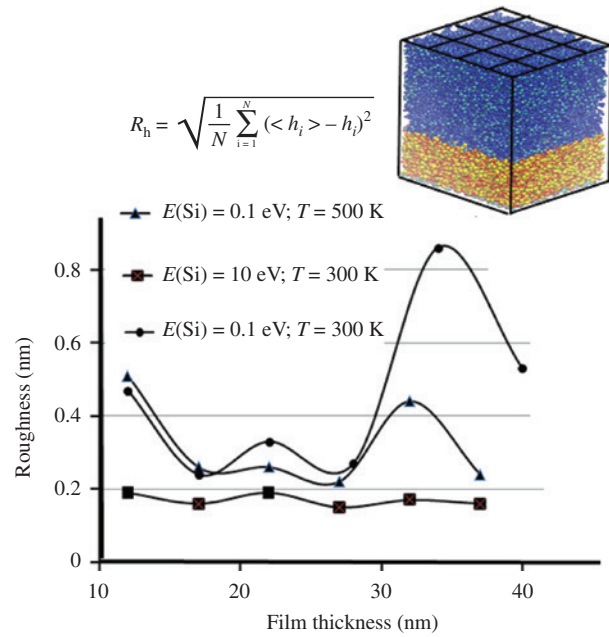
4.2 Roughness

In Ref. [62], the surface roughness was calculated as a root mean square deviation of the vertical coordinates of the surface atoms. The surface roughness of the deposited TIO_2 films was calculated in Ref. [3] using the kMC approach. In all the cases, the roughness was increased with the growth of the number of the deposited atoms, and it achieved 1.5 nm for N = 2 · 10^6. The roughness was also increased with the growth of the angle of incidence. It was reduced from 1.3 nm to 0.2 nm with an increase in the deposited Ti atom energy from 0.1 eV to 10 eV (angle of incidence equal to zero).

The dependence of the roughness R_h on the SIO_2 thin-film thickness and deposition conditions was investigated in the frame of the DESIL force field in Refs. [10–14]. To calculate R_h, the horizontal plane of the simulation box was divided into square cells having the same surface areas (see Figure 4). For every cell, a search for the atom with a maximum vertical coordinate h_i was performed.

The R_h value was then calculated as a rms of the h_i values. The calculated R_h values were in a good agreement with the experimental data [63]. It is seen from Figure 4 that the decrease in the substrate temperature results in the increase in the R_h values in the case of the silicon atom energy of 0.1 eV. The growth of the deposition energy leads to a reduction in the surface roughness.

The theoretical models of the evolution of the surface characteristics including the roughness characteristics are discussed in Ref. [53]. The horizontal plane of the growing film was divided into cells. The equations describing the time dependence of the film height in the frame of every cell were derived. The model taking into account surface diffusion was applied in studying the diamond-like carbon film growth. It was found that the increase in the deposition energy leads to the decrease in the surface roughness.

$$R_h = \sqrt{\frac{1}{N} \sum_{i=1}^{N} (<h_i> - h_i)^2}$$

Figure 4: Dependencies of thin-film roughness on film thickness for various energies of deposited Si atoms E(Si) and different substrate temperatures T.

4.3 Porosity and point defects

The porosity analysis of the TIO_2 films was performed in Refs. [3, 44]. The kMC approach was used to obtain a film cluster consisting of two million deposited atoms. Only the pores that were able to contain at least 15 atoms were taken into account. It was found that the closed pores were located near the growing film surface, and this was considered as the evidence of a rather dense structure of the film. The total volume of all the closed pores having diameters of at least two atomic dimensions was found to be equal to 7% of the total cluster volume. The pore concentration rapidly decreased with the pores size growth.
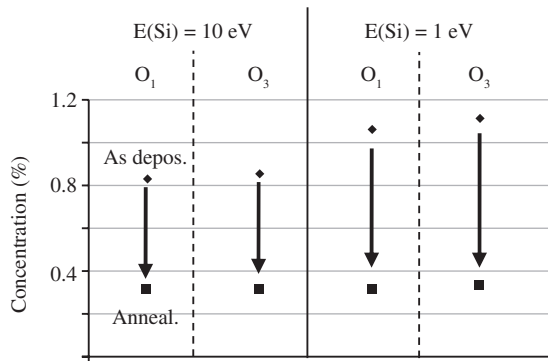
The porosity of the silicon dioxide films was studied in the frame of the classical MD simulation using the DESIL force field in Refs. [10–14]. The number of the deposited atoms in the simulation procedure achieved 2.4 · 10^5.

Only the pores having dimensions of at least 0.1 nm were taken into account. It is seen from Figure 5 that low deposition energy results in the formation of pores with dimensions of up to several nanometers. These pores are not observed in the case of high deposition energy. The concentration of the pores for all dimensions is reduced with the growth of the deposition energy.

The simulation of the point defects in the silicon dioxide thin films and fused silica was performed in Ref. [14]. It was found that the main types of point defects in
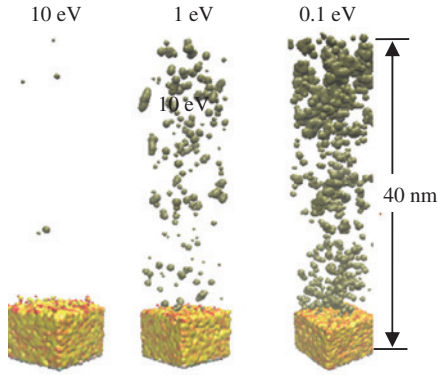
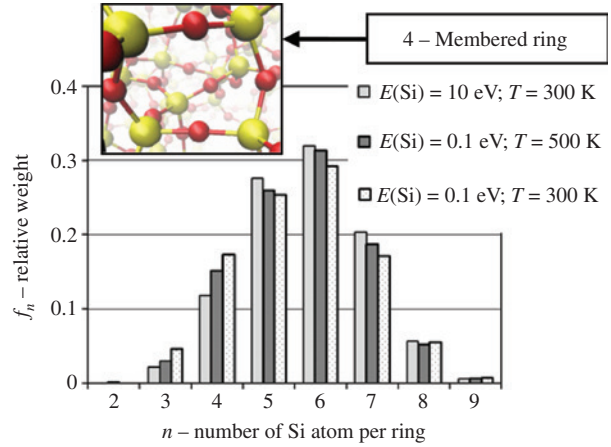**Figure 5:** Pores in the SIO$_2$ films atomistic structure. Values of the deposited Si atom energies are shown.

Figure 7: Ring statistic for different deposition conditions.

Figure 6: Point defect concentration in 'as-deposited' and annealed SIO$_2$ films.

SiO$_2$ were one- and three-coordinated oxygen atoms O$_1$ and O$_3$. The concentrations of these defects were calculated for the two films deposited at different energies of the deposited Si atoms. The influence of annealing on the point defect concentration was also studied. The results are shown in Figure 6. The defect concentration in the 'as-deposited' films is higher in the case of low deposition energy. The annealing procedure results in the essential reduction of the point defect concentration for all defect types and for all deposition energies.

4.4 Ring statistics

Rings consisting of different numbers of atoms (n-membered rings) are formed in different compounds (SiO$_2$, TiO$_2$, B$_2$O$_3$, and so on). The relative weights of the n-membered rings is defined as $f_n = N_n/N_{tot}$, where N_n is the number of the n-membered rings and N_{tot} is the total number of rings.

The relative weights for the different n were calculated for the deposited SiO$_2$ films using the MD approach with the DESIL force field. The crystalline silicon dioxide consists of only six- and eight-membered rings, while in the fused silica and SiO$_2$ films, rings with different n values are formed. Values of f_n were calculated using the shortest path analysis [64].

The results of the ring statistic calculations are shown in Figure 7. The geometry of the chemical bonds is strained in the rings with $n < 5$ as the values of the interatomic Si−O distances and the valence angles O−Si−O differ from the equilibrium ones. The most strained structure is formed in the case of the low substrate temperature and low energy of the deposited Si atoms.

The obtained distributions of the f_n values are in agreement with the experimental results for the fused silica [65, 66]. The detailed comparison of the f_n distribution for the different force fields is performed in Ref. [67]. For all the force fields, the distribution maximum corresponds to the six-membered ring. The relative weight of the strained rings (N < 5) is minimal in the case of the Tersoff potential for SiO$_2$ [30].

5 Mechanical properties

The Classical MD (MC) simulation enables one to study such important thin-film properties as its stress. The tensile and compressive types of stress are schematically shown at the top of Figure 8; their values have positive and negative signs, respectively. Stress can be calculated using the diagonal components of the pressure tensor p_{xx}, p_{yy} at the boundaries of the modeling box (the film grows in the z direction). These components are calculated based on the difference of the kinetic energies of the system and its virial. The values of p_{xx} and p_{yy} are averaged over
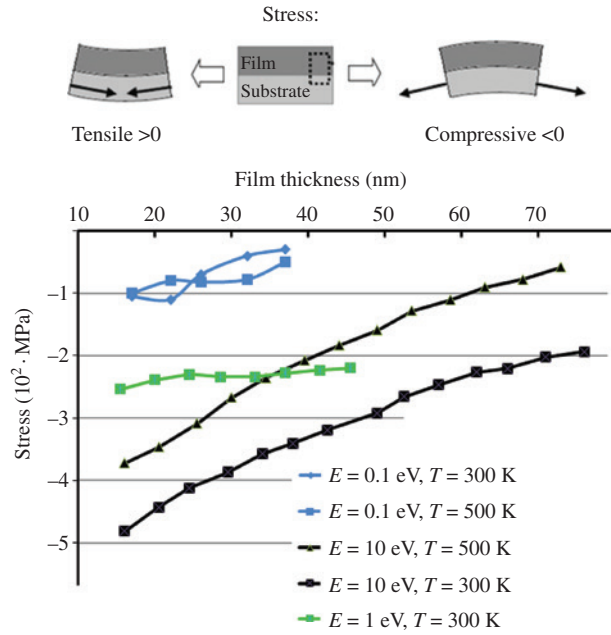
Figure 8: Dependencies of the stress on film thickness for different energies *E* of deposited Si atoms and substrate temperatures *T*.

the MD trajectories in the NVT (constant number of particles, volume, and temperature) ensemble with $T = 300$ K after the deposition process is finished. The diagonal components of the stress tensor $\sigma_{xx(yy)}$ are calculated as $\sigma_{xx(yy)} = -p_{xx(yy)}$.

The results of the stress simulation for silicon dioxide thin films using the DESIL force field are shown in Figure 8. Only the average values of the horizontal plane diagonal stress component $\sigma = (\sigma_{xx} + \sigma_{yy})/2$ are presented because the differences between σ_{xx} and σ_{yy} are small for all the values of film thickness.

In all cases, the compressive stress is observed. In the case of the deposited Si atom energy $E = 10$ eV, the absolute stress value is several times larger than in the case of $E = 0.1$ eV. The growth of the substrate temperature results in the reduction of stress in the case of $E = 10$ eV. The calculated stress values are in a good agreement with the experimental data [68].

The value of the mechanical loss in thin films is the limiting factor for high-precision gravitational wave detectors and optical devices that are used in the laser interferometer gravitational-wave observatory project. The two-well model is used to calculate the dependence of the mechanical loss in optical coatings on temperature and frequency in amorphous pure and doped silica [69] and amorphous tantala and titania-doped tantala [70]. The functional form of the interatomic potential energy was corresponded to the BKS potential [21] with an additional Morse term. The force field parameters were fitted

to repro duce the radial distribution functions and elastic constants. The low-temperature peaks in the loss of pure and doped tantala were reproduced in the simulation.

6 Optical and electronic properties

The dependence of the electronic HOMO-LUMO gap of the amorphous TiO_2 on the mass density was investigated in Ref. [16] using the DFTB approach [52] and the VASP quantum molecular dynamics program [48]. It was found that the gap decreases almost linearly with the increase in the mass density.

The dependencies of the refractive index n on the energy of the TiO_2 supercell and on the number of atoms in the supercell are studied in Ref. [9]. It was found that n increases with the growth of energy. The calculated value of n was less than the experimental one for 0.2 in the visible spectral range.

The densities of the deposited silicon dioxide films are higher than the fused silica density (see Table 1). This results in the respective growth of n. The difference Δn between the refractive indexes of the film and the glassy SiO_2 was estimated using the Gladstone-Dale equation [71] in the form $\Delta n = 0.21 \cdot \Delta\rho$, where $\Delta\rho$ is the difference between the film and glassy density. For the 'as-deposited' film at $E(Si) = 10$ eV, the value of Δn achieves 0.05. The annealing procedure results in the essential reduction of $\Delta\rho$ and, respectively, of Δn. The values of the densities and refractive indices that were obtained by the MD simulation with the DESIL force field are in agreement with the experimentally reported values [72].

The experimental verification of the validity of the SiO_2 deposition simulation is performed in Ref. [73]. The refractive index dependence on the wavelength is shown in Figure 9. It is seen that the refractive index difference between the glassy silicon dioxide and the SiO_2 film is
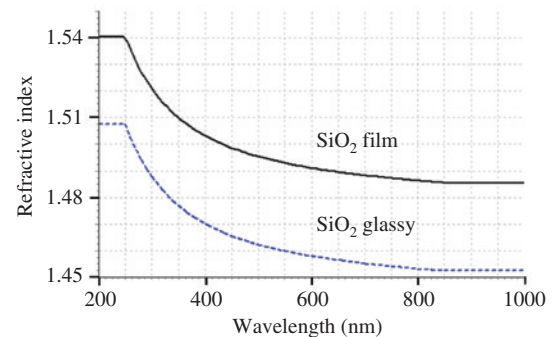
Figure 9: Experimental dependencies of the refractive index on wavelength for the silicon dioxide glassy and deposited film.

close to 0.04 for all wavelengths in the considered diapason. This result corresponds to the calculated Δn value in the case of the deposited Si atom energy 10 eV.

7 Conclusion

The methods of the simulation of the structural, mechanical, electronic, and optical properties of the deposited films are discussed. Special attention is paid to the atomistic simulation, as quantum as classical. The classical molecular dynamic modeling of the structural and mechanical film properties is considered in detail. The simulation results relating to the dependencies of film density, point defect concentration, stresses, surface roughness, porosity, refractive index, and gap in the density of the electronic states on the deposition conditions are observed. Application of the considered approaches to the simulation of silicon dioxide film deposition is discussed in detail. The increase in the energy of the deposited Si atoms results in the increase in the silica film density and the decrease in the porosity and the growth of absolute values of compressive stress.

References

[1] M. Sikkens, I. J. Hodgkinson, F. Horowitz, H. A. Macleod and J. J. Warton, Proc. SPIE 505, 236 (1984).

[2] M. Sikkens, I. J. Hodgkinson, F. Horowitz, H. A. Macleod and J. J. Wharton, Opt. Eng. 25, 142 (1986).

[3] M. Turowski, M. Jupé, T. Melzig, P. Moskovkin, A. Daniel, et al., Thin Solid Films 592, 240 (2015).

[4] N. Metropolis and S. Ulam, J. Am. Stat. Assoc. 44, 335 (1949).

[5] F. Grigoriev, A. Sulimov, I. Kochikov, O. Kondakova, V. Sulimov, et al., Optical Interference Coatings (OIC) 2016 © OSA 2016. WB.5.pdf

[6] E. C. Neyts and A. Bogaerts, in: 'Theoretical Chemistry in Belgium. Highlights in Theoretical Chemistry', Eds. By B. Champagne, M. Deleuze, F. De Proft and T. Leyssens, vol 6. (Springer, Berlin, Heidelberg, 2014).

[7] M. Taguchi and S. Hamguchi, Jpn. J. Appl. Phys. 45 (10B), 8163 (2006).

[8] M. Taguchi and S. Hamaguchi, Thin Solid Films 515, 4879 (2007).

[9] M. Turowski, T. Amotchkina, H. Ehlers, M. Jupé and D. Ristau, Appl. Opt. 53, A159 (2014).

[10] F. V. Grigoriev, A. V. Sulimov, I. V. Kochikov, O. A. Kondakova, V. B. Sulimov, et al., Int. J. High Perform. Comp. Appl. 29, 184 (2015).

[11] F. Grigoriev, Moscow University Physics Bulletin 70, 521 (2015).

[12] F. V. Grigoriev, A. V. Sulimov, I. V. Kochikov, O. A. Kondakova, V. B. Sulimov et al., Proc. SPIE. 9627, 962708 (2015).

[13] F. V. Grigoriev, A. V. Sulimov, E. V. Katkova, I. V. Kochikov, O. A. Kondakova, et al., J. Non-Cryst. Solids 448, 1 (2015).

[14] F. V. Grigoriev, E. V. Katkova, A. V. Sulimov, V. B. Sulimov, I. V. Kochikov, et al., Opt. Mater. Exp. 6, 3960 (2016).

[15] F. Grigoriev, A. Sulimov, I. Kochikov, O. Kondakova, V. Sulimov, et al., Appl. Opt. 56, C87 (2017).

[16] T. Köhler, M. Turowski, H. Ehlers, M. Landmann, D. Ristau, et al., J. Phys. D: Appl. Phys. 46, 325302 (2013).

[17] V. Georgieva, M. Saraiva, N. Jehanathan, O. I. Lebelev, D. Depla, et al., J. Phys. D: Appl. Phys. 42, 065107 (2009).

[18] A. Takada, P. Richet, C. R. A. Catlow and G. D. Price, J. Non-Cryst. Solids 345, 224 (2004).

[19] N. T. Huff, E. Demiralp, T. Cagin and W. A. Goddard III, J. Non-Cryst. Solids 253, 133 (1999).

[20] T. Soules, G. H. Gilmer, M. J. Matthews, J. S. Stolken and M. D. Feit, SPIE 2010 Boulder, 1–34 (2010) (digital.library.unt.edu/ark:/67531/metadc871862/).

[21] B. W. H. van Beest, G. J. Kramer and R. A. van Santen. Phys. Rev. Lett. 64, 1955 (1990).

[22] C. R. A. Catlow, C. M. Freeman and R. L. Royle, Physica B and C 131, 1 (1985).

[23] P. M. Morse, Phys. Rev. 34, 57 (1929).

[24] H. N. G. Wadley, X. Zhou and R. A. Johnson, Prog. Mater. Sci. 46, 329 (2001).

[25] V. V. Hoang, N. T. Hai and H. Zung, Phys. Lett. A 356, 246 (2006).

[26] A. Bahramian, Surf. Interface Anal. 45, 1727 (2013).

[27] L. Xie, P. Brault, J.-M. Bauchire, A.-L. Thomann and L. Bedra, J. Phys. D: Appl. Phys. 47, 224004 (2014).

[28] F. H. Stillinger and T. A. Weber, Phys. Rev. B 31, 5262 (1985).

[29] H. Ohta and S. Hamaguchi, J. Chem. Phys. 115, 6679 (2001).

[30] S. Munetoh, T. Motooka, K. Moriguchi and A. Shintani, Comput. Mater. Sci. 39, 334 (2007).

[31] M. Matsui and M. Akaogi, Mol. Simul. 6, 239 (1991).

[32] L. J. Vernon, R. Smith and S. D. Kenny, Nucl. Instrum. Methods B 267 3022 (2009).

[33] L. J. Vernon, S. D. Kenny and R. Smith, Nucl. Instrum. Methods B 268, 2942 (2010).

[34] Y. Yu, B. Wang, M. Wang, G. Sant and M. Bauch, J. Non-Cryst. Solids 443, 148 (2016).

[35] A. Carre, J. Horbach, S. Ispas and W. Kob. EPL 82, 17001 (2008).

[36] D. Corradini, Y. Ishii, N. Ohtori and M. Salanne. Modelling Simul. Mater. Sci. Eng. 23, 074005 (2015).

[37] Y. Maekawa and Y. Shibuta, Chem. Phys. Lett. 658, 30 (2016).

[38] C. T. Adri van Duin, A. Strachan, S. Stewman, Q. Zhang, X. Xu, et al., J. Phys. Chem. A 107, 3803 (2003).

[39] C. T. Adri van Duin, S. Dasgupta, F. Lorant and W. A. Goddard, III. J. Phys. Chem. A 105, 9396 (2001).

[40] C. T. Adri van Duin, J. M. A. Baas and B. van de Graaf. J. Chem. Soc., Faraday Trans. 90, 2881 (1994).

[41] H. J. C. Berendsen, J. P. M. Postma, W. F. van Gunsteren, A. DiNola and J. R. Haak. J. Chem. Phys. 81, 3684 (1984).

[42] T. Darden, D. York and L. Pedersen. J. Chem. Phys. 98, 10089 (1993).

[43] S. Lucas and P. Moskovkin, Thin Solid Films 518, 5355 (2010) (NASCAM available for downloading at http://www.unamur. be/sciences/physique/pmr/telechargement/logiciels/ nascam).

[44] V. Godinho, P. Moskovkin, R. Alvarez, J. Caballero-Hernandez, R. Schierholz, et al., Nanotechnology 25, 355705 (2014).

[45] Z. Peifeng, Z. Xiaoping and H. Deyan, Sci. China (Series G) 46, 610 (2003).

[46] M. Pomeroy, J. Joachim and C. Colin, Phys. Rev. B 66, 235412-1 (2002).

[47] H. L. Wei, Z. L. Liu and K. L. Yao, Vacuum 56, 185 (2000).

[48] G. Kresse and J. Furthmüller. Comput. Mater. Sci. 6, 15 (1996).

[49] P. Hohenberg, Phys. Rev. 136, B864 (1964).

[50] J. P. Perdew, K. Burke and M. Ernzerhof, Phys. Rev. Lett. 77, 3865 (1996).

[51] J. Heyd, G. E. Scuseria and M. Ernzerhof, J. Chem. Phys. 118, 8207 (2003).

[52] M. Elstner, T. Frauenheim and S. Suhai, J. Mol. Struct. (Theochem) 632, 29 (2003).

[53] F. L. Forgerini and R. Marchiori, Biomatter 4, e28871 (2014).

[54] E. F. da Silva and B. D. Stosi, Semicond. Sci. Technol. 12, 1038 (1997).

[55] M. Turowski, M. Jupé, H. Ehlers, T. Melzig, A. Pflug, et al., Proc. SPIE 9627, 962707 (2015).

[56] H. J. C. Berendsen, D. van der Spoel and R. van Drunen, Comput. Phys. Commun. 91, 56 (1995).

[57] W. Smith and T. Forester, J. Mol. Graph. 14, 136 (1996).

[58] T. F. Soules, G. H. Gilmer, M. J. Matthews, J. S. Stolken and M. D. Feit, J. Non-Cryst. Solids 357, 1564 (2011).

[59] V. V. Hoang, J. Phys. Chem. B 111, 12649 (2007).

[60] K. Taniguchi, M. Tanaka, C. Hamaguchi and K. Imai, J. Appl. Phys. 67, 2195 (1990).

[61] A. Roder, W. Kob and K. Binder, J. Chem. Phys. 114, 7602 (2001).

[62] E. S. Gadelmawla, M. M. Koura, T. M. A. Maksoud, I. M. Elewa and H. H. Soliman, J. Mater. Process. Technol. 123, 133 (2002).

[63] F. Elsholz, E. Schöll, C. Scharfenorth, G. Seewald, H. J. Eichler, et al., J. Appl. Phys. 98, 103516 (2005).

[64] X. Yuan and A. N. Cormack, Comput. Mater. Sci. 24, 343 (2002).

[65] Y. Tu and J. Tersoff, Phys. Rev. Lett. 84, 4393 (2000).

[66] V. M. Burlakov, G. A. D. Briggs, A. P. Sutton and Y. Tsukahara, Phys. Rev. Lett. 86, 3052 (2001).

[67] S. von Alfthan, A. Kuronen and K. Kaski, Phys. Rev. B 68, 073203 (2003).

[68] W. J. Fang, Micromech. Microeng. 9, 230 (1999).

[69] R. Hamdan, J. P. Trinastic and H. P. Cheng, J. Chem. Phys. 141, 054501 (2014).

[70] J. P. Trinastic, R. Hamdan, C. Billman and H.-P. Cheng, Phys. Rev. B 93, 014105 (2016).

[71] K. Vedam and P. Limsuwan, J. Chem. Phys. 69, 4772 (1978).

[72] Y. Jiang, H. Liu, L. Wang, D. Liu, C. Jiang, et al., Appl. Opt. 53, A83 (2014).

[73] V. G. Zhupanov, F. V. Grigoriev, V. B. Sulimov and A. V. Tikhonravov, Mosc. Univ. Phys. Bull. 72, (2017).

Fedor Grigoriev
Research Computing Center, Moscow State University, Leninskie Gory, 119992 Moscow, Russia, e-mail: fedor.grigoriev@gmail.com

Fedor Grigoriev is Senior Research Scientist of the Research Computing Center M. V. Lomonosov Moscow State University. He graduated from the Faculty of Theoretical and Experimental Physics at the National Research Nuclear University (MEPhi) in 1994. He obtained his PhD degree in Physical Chemistry from Kurnakov Institute of General and Inorganic Chemistry, Russian Academy of Sciences. He is an author of more than 50 publications. His research interests are the atomistic supercomputer simulation of the processes of the thin-film deposition, formation of the interatomic complexes in water, and formation of the point defects in solid phase.

Vladimir Sulimov
Research Computing Center, Moscow State University, Leninskie Gory, 119992 Moscow, Russia

Vladimir Sulimov is presently the Head of the laboratory of the Research Computing Center of Lomonosov Moscow State University, Moscow, Russia. He obtained his PhD degree in Mathematical and Theoretical Physics from Lomonosov Moscow State University and his Doctor of Sciences degree in Mathematical and Theoretical Physics from Prokhorov General Physics Institute of Russian Academy of Sciences. He is an author of more than 240 publications. His current research interests are in the application of molecular modeling to solving a broad spectrum of problems, including computer-aided structural-based drug design and thin optical film deposition modeling, application of Bayesian network technology to personalized medicine, and application of high-performance computing to these problems.

Alexander Tikhonravov
Research Computing Center, Moscow State University, Leninskie Gory, 119992 Moscow, Russia

Alexander Tikhonravov is presently the Director of the Research Computing Center of Moscow State University, Moscow, Russia. He obtained his PhD degree and his Doctor of Sciences degree in Mathematical and Theoretical Physics from Moscow State University. He is an author of more than 350 publications. His current research interests are in thin-film optics, inverse problems, and application of high-performance computing to challenging technological problems.